

Chest Radiographic Findings in High-risk Covid-19 Pneumonia Patients

Iroshani Kodikara (✉ iroshani.kodikara@gmail.com)

University of Ruhuna Faculty of Medicine <https://orcid.org/0000-0001-8534-4571>

Buddhi Anjani Galabada

Base Hospital Homagama, Sri Lanka

Aruni Manjula Kurupparachchi

Base Hospital Homagama, Sri Lanka

Research Article

Keywords: Covid-19 pneumonia, high risk patients, chest X-ray features, temporal progression

Posted Date: January 13th, 2022

DOI: <https://doi.org/10.21203/rs.3.rs-1210242/v1>

License: © ⓘ This work is licensed under a Creative Commons Attribution 4.0 International License.

[Read Full License](#)

Abstract

Background/ objectives

The severity of Covid-19 pneumonia has shown a positive association with co-existing risk factors. However, the exact nature of lung involvement in high-risk Covid-19 patients is yet to be resolved. Therefore, we evaluated the CXR features, temporal progression, and the factors associated with CXR severity in high-risk patients.

Methods

Chest X-rays (n=289) of Covid-19 infected high-risk adults (n=228) treated at the Base Hospital Homagama were evaluated to record CXR features, their temporal progression, CXR severity score and the patient outcomes.

Results

The studies patients (48.2% men) were in mean age(SD) of 59(15) years. The most frequent CXR features were patchy ground-glass opacities (49%; GG) and patchy consolidations (42%; CON). They showed bilateral (100%) involvement, superoinferior gradient (100%) and diffuse (27%), peripheral (18%) or perihilar (10%) distribution. CON was the predominant opacity among the non-survivors and GG among the survivors ($\chi^2=14.73$; $p=0.001$). Right lung predominant (28%) asymmetrical lung involvement was more frequent than bilateral symmetrical (16%) or left lung predominance (7%). Progression into fatal disease was significantly higher when the lung involvement is asymmetrical: right predominance: ODDs:0.502; $p=0.023$; left predominance: ODDs:0.268; $p=0.002$. The CXRs were frequently normal in early (66%) and progressive (56%; $\chi^2=36.64$; $p<0.001$) stages than in peak or resolving stages. The predictors of CXR severity included age ($\beta:0.140$; 95% CI:0.041–0.233; $p=0.004$), male gender ($\beta:4.140$; 95% CI:1.452–6.481; $p=0.003$), and disease day ($\beta:0.622$; 95% CI:0.301–0.942; $p<0.001$).

Conclusion

This study decoded the CXR features of Covid-19 pneumonia in a high-risk cohort while describing their associations.

Introduction

Covid-19 disease caused by the severe acute respiratory syndrome coronavirus-2 (SARS-CoV-2) principally affects the respiratory epithelium. Immunocompetent hosts mostly experience a mild infection confined to the upper respiratory tract [1]. However, a minority, with or without other risk factors, can progress into acute respiratory distress syndrome (ARDS) that need intensive care (ICU) management. Newly mutated viral strains such as the Delta variant are shown to have much higher virulence with frequent lower respiratory tract involvement [2, 3].

The diagnosis of severe Covid-19 disease is with clinical, biochemical and radiological investigations. Clinical features of critical lung involvement include increased work of breath, low peripheral oxygen saturation and increasing oxygen requirements. For clinically suspected severe disease, chest radiographs (CXR) and computed tomographic scans of the chest (CT) are employed to detect the extent of lung involvement [4, 5].

Despite the high sensitivity of CT in detecting lung pathology, on-site CXRs are helpful when CT facilities are unavailable or with practical difficulties for critically ill patient mobilization [5, 6]. Among other features, bilateral-symmetrical lower zone CXR opacities have been described as the most common pattern in Covid-19 pneumonia. The CXR severity score has been recognized as a reliable risk predictor [6, 7, 8, 9, 10, 11, 12].

A strong correlation has been described between the severity of Covid-19 pneumonia and co-existing risk factors [2, 9, 10]. Since most available studies focused on lung involvement in otherwise healthy adults, the lung involvement patterns in high-risk patients are yet to understand. Geographical or ethnic factors have also shown an association with the severity of Covid-19 lung disease. Therefore, more population-based studies are warranted to recognize the true nature of this novel infection [13]. Precisely, the knowledge gap on lung involvement patterns of high-risk Covid infected patients has to fulfil.

Since the first report of Covid-19 infected patients from Sri Lanka, diagnosed patients are managed in health care facilities as in-patients. The study centre functions as a dedicated national multidisciplinary treatment centre catering for the entire country that admits high risk, symptomatic Covid patients. Therefore, the study centre provides an excellent opportunity to study a cohort of high risk symptomatic Covid-19 patients.

Thus, this study aimed to describe the CXR features and their temporal sequence of high-risk Covid infected patients. And to identify the factors associated with CXR severity.

Methods

This study has evaluated the chest radiographs (CXR) of Covid-19 infected adult (age >18 years) patients (n = 228) treated at the Base Hospital Homagama from 1st of December 2019 to 1st of February 2020. The Covid-19 diagnosis was made either by positive RT-PCR or rapid antigen test to detect SARS COV 2 antigen. The patient details - socio-demographic data; details of current presentation; previous comorbidities; risk factors; outcome; the date of diagnosis - were retrospectively extracted from the records. The ethical clearance for the study was granted by the Ethical Review Committee of Sri Lanka Medical association (Protocol No: ERC/21-001).

The CXRs have been obtained using the same portable X-ray unit as anteroposterior (AP) or supine projection. These CXRs were evaluated by two experienced Radiologists (experienced for more than seven years) under the same image viewing conditions. The CXRs were reported on consensus agreement. Based on the clinical and radiographic features, the CXRs were categorized as normal/ abnormal or

changes of Covid-19 lung disease/ non-Covid lung disease. The patients (n = 73) who had indeterminate CXR features, poor image quality or were suggestive of associated comorbidity/ pre-existing lung disease were excluded from the study.

The CXR opacities were categorized as follows using the Fleischner society glossary [14]. consolidation (patchy/lobar or segmental), ground-glass opacities (GGO), reticulation/interstitial thickening, atelectasis, pulmonary nodules, pleural effusion, hilar lymphadenopathy, lung cavitation, reverse halo sign, or pneumothorax. The distribution of CXR opacities was categorized: 1. peripheral, peri-hilar predominance or diffuse; 2. right, left, bilateral lung involvement; 3. upper, mid and lower zone involvement. The peripheral and peri-hilar demarcation was made by drawing an imaginary line midway between the lateral lung edge and hilum - the area medial to the line was considered peri-hilar.

The CXR severity was defined using a validated severity score [15]. The lung was divided into three zones by drawing two horizontal lines - just below the aortic arch and right pulmonary vein. A score was allocated for each zone considering the area involved (score 0 = no involvement; 1 \leq 25%; 2 = 25–50%; 3 = 50–75%; 4 \geq 75% area involvement) and the predominant density pattern (score 1 = ground glass/reticular opacity; score 2 = consolidation). The severity score for each lung zone (upper, middle, and lower zones) was calculated by multiplying the scores obtained for the area involved and density. The total score of each patient is ranged from 0 to 48. A CXR severity grade was assigned using the total severity scores of the patient: mild - severity score 1 to 16; moderate – 17 to 32; severe – 33 to 48.

The temporal progression of CXR features was assessed by considering the date of diagnosis as day 0. Disease stages were categorized as stage 1 or early stage (0 to 4 days); stage 2 or progressive stage (5 to 8 days); stage 3 or peak stage (9 to 13 days); and stage 4 or resolving stage (\geq 14 days).[16]

Statistical method

Once confirming the normalcy of the data set, parametric analysis was done. Continuous variables were expressed as means and standard deviations and categorical variables as percentages. The groups were compared with one-way ANOVA, T-test, Chi-square analysis and linear regression analysis. A P-value less than 0.05 was considered significant.

Results

Patient characteristics

The 228 Covid-19 infected patients (48.2% men) included in the study were in the mean age (SD) of 59 (15) years, and a range of 18 to 87 years. Table 01 describes the baseline characteristics of the study cohort. Of them, 89.5% have discharged uncomplicated, while 17.1% had a fatal outcome. In this high-risk cohort, most patients (85%) have had at least one coexisting disease, which raised to 92.3% among the non-survivors.

Table 01
Baseline characteristics of the study population

	All (n = 228)	Non-survivors (n = 39)	Survivors (n =189)
Age (SD)	59 (15)	61 (12)	59 (15)
Gender			
Male	110 (48.2%)	24 (61.5%)	86 (45.5%)
Female	118 (51.8%)	15 (38.5%)	103 (54.5%)
Ethnicity			
Sinhala	147 (64.5%)	24 (61.5%)	123 (65.1%)
Muslim	53 (23.2%)	11 (28.2%)	42(22.2%)
Tamil	26 (11.4%)	3 (7.7%)	23 (12.2%)
Other	1 (0.4%)	0 (0%)	1 (0.5%)
Smoking			
Yes	12 (5.3%)	2 (5.1%)	10 (5.1%)
No	214 (93.9%)	36 (92.3%)	178 (94.2%)
Comorbidities			
Yes	194 (85.1%)	36 (92.3%)	158 (83.6%)
No	33 (14.5%)	2 (5.1%)	31 (16.4%)
>2	92 (40.7%)	22 (56.4%)	70 (37%)
Days from diagnosis mean (range)	7 (1 – 21)	8 (1 – 19)	6 (1 – 21)
SpO2	95%	92%	96%
Low SPO2 (<95%)	82 (37.3%)	26 (66.7%)	56 (29.6%)

Chest x-ray features

Excluding 73 patients of whom the CXR features were either non-conclusive, features of pre-existing lung disease or associated comorbidity, 289 CXRs of 228 patients have evaluated to describe CXR features. Averagely, the chest imaging was done 7 days after the diagnosis (range of 1 to 21 days). Table 2 describes the CXR features of Covid-19 pneumonia: 49.1% of them had at least one normal CXRs in the

acute phase. Normal CXR was frequent among the survivors (55.7%; non-survivors 24.6%), while features of Covid-19 pneumonia were frequently present among the non-survivors (75.4% and 44.3% of survivors; $\chi^2=17.72$, $p<0.001$).

Figure 1 describes the CXR features of Covid-19 pneumonia identified in the study cohort. Patchy ground-glass opacities (49%; GG) and patchy consolidations (42%; CON) were the most frequent CXR findings of Covid-19 pneumonia (Table 02; Figure 1). Importantly, lobar or segmental consolidations were not present in the study cohort. Lung nodules, masses, hilar lymph nodes, pneumothorax and pneumomediastinum were not present in this study cohort. Compared to survivors, CON and GG were more frequent among non-survivors ($\chi^2=33.08$; $p<0.001$). Importantly, patchy CON was the predominant opacity pattern among non-survivors, whereas the GG was among the survivors ($\chi^2=14.73$; $p = 0.001$). Some features, such as reticular shadows, atelectatic bands and pleural effusions, have not shown an association with disease severity (Table 02).

Table 02
Distribution of radiographic features of Covid-19 pneumonia

CXR feature	All (n = 228)	Non- survivors (n = 39)	Survivors (n =189)	P value
Number of CXR	289	61	228	
CXR findings				
Normal	142 (49.1%)	15 (24.6%)	127 (55.7%)	<0.001†
Typical Covid 19	147 (50.9%)	46 (75.4%)	101 (44.3%)	<0.001†
Type of opacity n (%)				
Consolidation	120 (42%)	40 (66%)**	80 (35%)	<0.001†
Ground glass	141 (49%)	44 (72%)**	97 (43%)	<0.001†
Reticular	29 (10%)	4 (7%)	25 (11%)	0.095
Atelectatic bands	10 (4%)	2 (0.3%)	8 (0.4%)	0.153
Pleural effusions	2 (0.7%)	1 (1.6%)	1 (0.4%)	0.092
Nodules	0 (0%)	0 (0%)	0 (0%)	-
Masses	0 (0%)	0 (0%)	0 (0%)	-
Lymphadenopathy	0 (0%)	0 (0%)	0 (0%)	-
Predominant opacity pattern				
Consolidation	71 (25%)	33 (54%)*	38 (17%)	0.001†
Ground glass	58 (20%)	10 (16%)	48 (21%)	
Reticular	18 (6%)	3 (5%)	15 (7%)	
Distribution of opacities n (%)				
Both lung	157 (100%)	46 (100%)	201 (100%)	0.467†
Bilateral symme.	46 (16%)	12 (20%)	34 (15%)	0.367†
RL pred.	80 (28%)	24 (39%)*	56 (25%)	0.022†
LL pred.	20 (7%)	10 (16%)*	10 (4%)	0.001†

(*p<0.05; **p<0.001; †: Chi-square analysis)

CXR feature		All (n = 228)	Non- survivors (n = 39)	Survivors (n =189)	P value
	Peripheral pred.	50 (18%)	12 (20%)**	38 (16.6%)	<0.001†
	Perihilar pred.	29 (10%)	7 (12%)**	22 (9.6%)	<0.001†
	Diffuse	78 (27%)	32 (53%)**	46 (20%)	<0.001†
	Lobar	0 (0%)	0 (0%)	0 (0%)	-
	Segmental	0 (0%)	0 (0%)	0 (0%)	-
Lobar involvement					
n (%)	Right upper zone	99 (34%)	31 (51%)**	68 (30%)	<0.001†
	Right mid zone	142 (49%)	44 (72%)**	97 (43%)	<0.001†
	Right lower zone	143 (50%)	46 (76%)**	97 (43%)	<0.001†
	Left upper zone	76 (25%)	24 (39%)**	48 (21%)	<0.001†
	Left mid zone	134 (45%)	43 (71%)**	88 (39%)	<0.001†
	Left lower zone	143 (50%)	45 (74%)**	98 (43%)	<0.001†
(*p<0.05; **p<0.001; †: Chi-square analysis)					

The lung opacities have shown a bilateral (100%) involvement with diffuse (27%), peripheral (18%) or perihilar (10%) distribution (Figure 1). Interestingly, unilateral lung involvement was not present in this study cohort. Anyhow asymmetrical lung involvement with a right-lung predominance (28%) was more frequent than bilateral symmetrical (16%) or left lung-predominant patterns (7%; Table 02). This distribution was confirmed again by showing a higher severity score in the right lung (5/48±6.3; left lung: (4.3/48±5.7; T = 5.3/48; p<0.001; Figure 2). The severity scores of right upper (T = 5.240; p<0.001), mid (T = 4.158; p<0.001) and lower zones (T = 2.908; p<0.001) were also significantly higher than those of left lung (Figure 2, Table 03). The progress into the fatal disease was significantly higher in asymmetrical lung involvement: right predominance: ODDs 0.502; p=0.023; left predominance: ODDs 0.268; p=0.002.

Table 03
Distribution of radiographic severity in Covid-19 pneumonia

Severity of CXR		All (n = 228)	Non-survivors (n = 39)	Survivors (n = 189)	P value
Number of CXR		289	61	228	
Area involved					
Right lung	No opacities	142 (49.1%)	15 (24.6%)	127 (55.7%)	<0.001†
	<25%	12 (4%)	1 (2%)	11 (5%)	
	25 – 50%	41 (14%)	10 (16%)	31 (14%)	
	50 – 75%	68 (24%)	16 (26%)	52 (23%)	
	>75%	25 (9%)	18 (30%)	7 (3%)	
Area involved					
Left lung	No opacities	142 (49.1%)	15 (24.6%)	127 (55.7%)	<0.001†
	<25%	12 (4%)	1 (2%)	11 (5%)	
	25 – 50%	55 (19%)	14 (23%)	41 (18%)	
	50 – 75%	57 (20%)	14 (23%)	43 (19%)	
	>75%	22 (8%)	16 (26%)	6 (3%)	
Severity score					
mean (SD)	Right lung	5.0 (6.3)	8.9 (7.2) **	4.0 (5.6)	<0.001€
	Left lung	4.3 (5.7)	8.1 (7.0)**	3.3 (4.8)	<0.001€
	Right upper zone	0.9 (1.6)	1.7 (2.2) **	0.7 (1.4)	<0.001€
	Right mid zone	1.8 (2.3)	3.1 (2.7) **	1.5 (2.1)	<0.001€
	Right lower zone	2.3 (2.8)	4.1 (3.2) **	1.8 (2.5)	<0.001€
	Left upper zone	0.7 (1.4)	1.3 (2.0) **	0.5 (1.0)	<0.001€
	Left mid zone	1.5 (2.2)	3.0 (2.8)**	1.2 (1.8)	<0.001€
	Left lower zone	2.1 (2.6)	3.8 (3.0) **	1.6 (2.3)	<0.001€
	Total score	9.3 (11.6)	16.8 (13.5) **	7.2 (10.2)	<0.001€
CXR severity					
	Normal	141 (49%)	14 (23%)	127 (56%)	<0.001†

(*p<0.05; **p<0.001; †: Chi-square analysis performed; €: paired or independent sample T-test analysis performed)

Severity of CXR	All (n = 228)	Non-survivors (n = 39)	Survivors (n =189)	P value
Mild	73 (25%)	15 (25%)	58 (25%)	
Moderate	59 (20%)	22 (36%)	37 (16%)	
Severe	15 (5%)	9 (15%)	6 (3%)	

(*p<0.05; **p<0.001; †: Chi-square analysis performed; €: paired or independent sample T-test analysis performed)

There was a supero-inferior gradient in the severity of lung involvement; the lower lung zones were more severely affected (with high severity scores) than the upper zones (right lung T = 10.7; left lung T =11.3; p<0.001). This supero-inferior gradient in lung involvement was more obvious among the non-survivors (T = 6.886; p<0.001). The area of lung involvement has also been associated with disease severity. In 90% of the study cohort and among 90% of survivors, the area involved was less than 75%, it was seen only in 30% of non-survivors ($\chi^2 = 50.552$; p<0.001; Table 03). Similarly, the proportion of patients who were classified as having a severe radiographic grade was significantly higher in the non-survived group (15%; survived group: 3%; $\chi^2 = 33.806$; p<0.001).

Table 04 describes the CXR features according to the disease stage. There was a clear temporal sequence in the distribution of CXR features. The CXRs were frequently normal in early (stage 1: 66%) and progressive (stage 2: 56%; $\chi^2=36.64$; p<0.001) stages than in the peak and resolving stages (Figure 3a). With the disease progression, the lungs were infiltrated with consolidation and ground-glass opacities (Figure 3a; consolidations: $\chi^2=24.27$; p<0.001; ground-glass opacities: $\chi^2=39.56$; p<0.001). Interestingly, reticular opacities were frequently present in the resolving phase (Table 03). The climax of lung involvement was found in the peak stage (stage 3) with a subsequent partial resolution in the resolving phase (stage 4; $\chi^2=37.76$; p<0.001; Figure 3c,d,e). In the early stages, opacities were predominantly present in the right lung. Later, they distributed to both lungs symmetrically (in stages 2 & 3). Again in the resolving phase (stage 4), the lung opacities were predominantly in the right lung ($\chi^2=12.51$; p=0.006). The peripheral and diffuse lung involvement have also increased with the disease progression (peripheral: $\chi^2=18.84$; p=0.004; diffuse: $\chi^2=17.71$; p=0.007; Table 04).

Table 04
Temporal sequence of chest X-ray features in Covid-19 pneumonia

Parameter	Stage 1 (113 CXRs)	Stage 2 (88 CXRs)	Stage 3 (50 CXRs)	Stage 4 (29 CXRs)	P value
Normal	75 (66%)	49 (56%)	11 (22%)	7 (24%)**	<0.001†
Infiltrates present	38 (34%)	39 (44%)	39 (78%)	22 (76%)	
Predominant opacity pattern					
Ground- glass	13 (12%)	19 (22%)	14 (28%)	8 (28%)**	<0.001†
Consolid.	21 (19%)	17 (19%)	19 (38%)	9 (31%)	
Reticular	4 (4%)	3 (3%)	6 (12%)	5 (17%)	
Distribution					
Peripheral	12 (11%)	13 (15%)	15 (30%)	6 (21%)*	0.004†
Perihilar	7 (6%)	8 (9%)	8 (16%)	5 (17%)*	0.025†
Diffuse	22 (20%)	22 (25%)	18 (36%)	12 (41%)*	0.007†
R/ lung pred.	26 (23%)	18 (21%)	16 (32%)	15 (52%)*	0.006†
L/ lung pred.	2 (2%)	4 (5%)	9 (18%)	4 (14%)*	0.001†
B/L symm.	10 (9%)	17 (19%)	14 (28%)	3 (10%)*	0.011†
Zonal involvement					
n (%)					
R/ upper	25 (22%)	26 (30%)	26 (52%)	17 (59%)**	<0.001†
R/ mid	37 (33%)	37 (42%)	38 (76%)	22 (76%)**	<0.001†
R/ lower	37 (33%)	39 (44%)	37 (74%)	22 (76%)**	<0.001†
L/ upper	15 (13%)	20 (23%)	21 (42%)	11 (38%)**	<0.001†

(†: Chi square analysis; *: p<0.05; **: p<0.001)

Parameter	Stage 1 (113 CXRs)	Stage 2 (88 CXRs)	Stage 3 (50 CXRs)	Stage 4 (29 CXRs)	P value
L/ mid	34 (30%)	34 (39%)	36 (72%)	20 (69%)**	<0.001†
L/ lower	38 (34%)	39 (44%)	36 (72%)	22 (76%)**	<0.001†

(†: Chi square analysis; *: p<0.05; **: p<0.001)

Irrespective of the disease stage, there was a supero-inferior gradient (100%) in the severity of lung involvement (range of T values=4.44 to 7.3; p<0.001). The upper lung zones involvement was more frequent in the late stages ($\chi^2=32.56$; p<0.001; Figure 3c). Similarly, the total severity scores and radiographic severity grades have increased progressively with the disease stage (Figure 3d & 3e). The highest severity score, area involved and CXR severity grade were seen in stage 3 (peak stage) that subsequently resolved in stage 4 (Table 05).

Table 05
Temporal sequence of chest severity in Covid-19 pneumonia

Parameter		Stage 1 (113 CXRs)	Stage 2 (88 CXRs)	Stage 3 (50 CXRs)	Stage 4 (29 CXRs)	P value
Area involved Right lung	0%	75 (66%)	50 (57%)	11 (22%)	6 (21%)**	<0.001†
	<25%	2 (2%)	2 (2%)	5 (10%)	0 (0%)	
	25 – 50%	10 (9%)	10 (11%)	12 (24%)	8 (28%)	
	50 – 75%	21 (19%)	20 (23%)	13 (26%)	11 (38%)	
	>75%	5 (4%)	6 (7%)	9 (18%)	3 (10%)	
Area involved Left lung	0%	75 (66%)	49 (56%)	12 (24%)	6 (21%)**	<0.001†
	<25%	3 (3%)	3 (3%)	3 (6%)	0 (0%)	
	25 – 50%	16 (14%)	12 (14%)	15 (30%)	10 (35%)	
	50 – 75%	14 (12%)	19 (22%)	12 (24%)	9 (31%)	
	>75%	5 (4%)	5 (6%)	8 (16%)	3 (10%)	
Severity score mean (SD)	Total score	6.0 (10)	7.2 (10)	15.3 (13)	14.1 (11)**	<0.001‡
	Right lung	3.4 (5.7)	4.0 (5.6)	8.0 (6.7)	7.9 (6.2)**	<0.001‡
	Left lung	2.6 (4.4)	3.2 (4.4)	7.3 (6.6)	6.9 (6.3)**	<0.001‡
	R/ upper	0.6 (1.5)	0.8 (1.5)	1.3 (1.7)	1.4 (1.6)*	0.016‡
	R/ mid	1.3 (2)	1.4 (2)	3.0 (2.5)	2.9 (2.4)**	<0.001‡
	R/ lower	1.5 (2.5)	1.7 (2.4)	3.8 (3.0)	3.5 (2.8)**	<0.001‡
	L/ upper	0.3 (1.0)	0.3 (1.3)	1.1 (1.7)	1.1 (1.6)*	0.001‡
	L/ mid	0.9 (1.6)	1.2 (1.8)	2.8 (2.6)	2.5 (2.5)**	<0.001‡
	L/ lower	1.4 (2.4)	1.5 (2.0)	3.4 (3.0)	3.3 (2.8)**	<0.001‡
CXR severity	Normal	75 (66%)	49 (56%)	11 (22%)	6 (21%)**	<0.001†
	Mild	19 (17%)	24 (27%)	17(34%)	10 (35%)	
	Moderate	16 (14%)	13 (15%)	16 (32%)	11 (38%)	

(‡: One way Anova analysis; †: Chi square analysis; *: p<0.05; **: p=<0.001)

Parameter	Stage 1 (113 CXRs)	Stage 2 (88 CXRs)	Stage 3 (50 CXRs)	Stage 4 (29 CXRs)	P value
Severe	3 (3%)	2 (2%)	6 (12%)	1 (3%)	
(‡: One way Anova analysis; †: Chi square analysis; *: p<0.05; **: p<0.001)					

A simple linear regression analysis was used to test the factors affecting the CXR severity. It was found that the age of the patient (β : 0.140; 95% CI: 0.041–0.233; p=0.004), male gender (β : 4.140; 95% CI: 1.452–6.481; p=0.003), and date since Covid-19 diagnosis (β : 0.622; 95% CI: 0.301–0.942; p<0.001) have significantly predicted the radiographic severity of Covid-19 pneumonia. In this model, the number of associated comorbidities (β : 0.340; 95% CI: -0.741–1.533; p=0.506) did not influence the radiographic severity of Covid-19 pneumonia.

Discussion

Covid-19, as a novel infectious disease, has created an enormous impact on global public health. Though new data are progressively available on different aspects of Covid-19 lung disease, still there is a scarcity of knowledge on CXR features and factors associated with CXR severity, particularly for high-risk groups. Covering this knowledge gap, in this study, we have described the CXR features of Covid-19 lung disease, their temporal sequence, and factors associated with radiographic severity, for a cohort of high-risk Covid-19 infected patients. The main CXR features of Covid-19 pneumonia detected in this study include consolidations and ground-glass opacities, which showed a supero-inferior gradient. Additionally, a temporal sequence of lung involvement has been established with the peak in the second week of illness. Also, the age of the patient and male gender were found as independent predictors of chest X-ray severity.

Many previous studies have recognized the factors associated with severe Covid-19 infection using risk un-stratified cohorts; associated comorbidity, male gender and ethnicity were among them [10, 12]. Considering the possible risk for progression of severe pneumonia into chronic lung injury, predicting and identifying the disease severity is valuable to anticipate subsequent chronic lung injury. Many previous studies have shown an association between risk factors and severe pneumonia; however, the small sample size was their limitation. Associated comorbidities such as diabetes, hypertension were the recognized risk factors for severe Covid-19 disease in the acute stage [17]. During the acute phase of illness, the consolidated lung volume (p=0.031) and proportion of lung involvement (p=0.019) among the Covid-19 infected diabetics (n=15) were significantly higher than that of non-diabetics (n=47).[17] A retrospective study done in Wuhan, China (n=41) reported a complication rate of 32% among the patients with associated comorbidity [18].

Similarly, we found a fatal outcome in 17.1% and radiographically severe disease in 50.9% in a cohort (n=228) with single or multiple risk factors. Thus, by studying a larger high-risk cohort, we confirm that the severity of lung infection is higher in the presence of risk factors. Notably, the limited experiences on post Covid follow up imaging raises the possibility of chronic lung disease in the high-risk patients and

patients with severe [19, 20]. Therefore, particularly for high-risk cohorts, imaging follow-ups may be necessary to detect Covid associated chronic lung disease early.

The Covid-19 pneumonia CXR features among the risk un-stratified cohorts included patchy consolidations, ground glass and reticular opacities [6, 8, 10, 21, 22]. Patchy consolidations favoured Covid-19 pneumonia, while lobar or segmental consolidations ruled out Covid lung disease [23]. Interestingly, the CXR opacities in Covid-19 pneumonia have shown a peripheral and lower lobe predominant distribution. Pleural effusion has been recognized as a rare feature [6, 8, 10, 21, 22, 24]. Cardiomegaly was described among the Covid infected patients without delineating a direct relationship to the coronavirus infection [6]. The CXR findings described in our high-risk cohort have also followed a similar pattern. Even though pulmonary nodules have occasionally been reported in Covid patients, none from the current study cohort have had pulmonary nodules [10, 21, 24]. The temporal progression of CXR features detected in this study was in agreement with previous studies done for risk un-stratified cohorts. The CXR features and severity scores have changed over time and peaked in the second week of infection [9]. All in all, the CXR features described in this study for a high-risk group were not different from the radiographic features of risk unstratified populations.

The CXR severity score has been correlated well with the patient outcome; the severity score has been increased with disease severity and fatality [7, 10, 24]. Irrespective of patients' risk status, there was a uniformity in finding lower lobe predominant lung involvement in Covid pneumonia [6, 7, 21, 24]. with a higher severity score in the lower zones. A similar pattern has been observed in this high-risk cohort as well. Therefore, severity score appears to be a reliable tool for risk stratification in high-risk patients as well.

In risk unstratified groups, most Covid infected patients had either a normal CXR or a CXR with mild severity [7]. Anyhow, as expected, we have not observed a hike in CXR severity grading in this high-risk cohort. Since previous CXR based studies have also included inward patients, though not mentioned clearly, their samples may have included at least a proportion of high-risk patients. These concealed overlaps in the study populations may have created comparable findings in high-risk and low-risk populations. Thus, comparing both high and low-risk patients using an adequate sample would be helpful to identify the actual burden of lung involvement in high-risk populations.

The lung involvement pattern in Covid 19 pneumonia has been described as bilateral symmetrical [6, 7, 21, 24]. However, recent studies have described a predominant right lung involvement pattern [7, 25]. We also noticed a right-predominant, asymmetrical lung involvement pattern more frequently than the bilaterally symmetrical pattern. Though it has been stated that the patients with right lung predominant disease were at a higher risk of hospitalization and a fatal outcome (OR = 2.662; p = 0.0252), our findings did not agree with it [25].

The strengths of this study design include evaluating a large sample exclusively from a high-risk cohort representing Sri Lankan population. Also the objective assessment of the CXR features with consensus

agreement of experienced observers increase the accuracy. However, a case-control study design would have further strengthened the study design.

Conclusion

The typical chest X-ray appearance and the temporal sequence of chest X-ray involvement identified in high-risk Covid-19 pneumonia patients closely follows the those of the risk un-stratified populations.

Declarations

Funding:

The data collection stage of this work was supported by the Ministry of Health Research Grant: ETR/M/MC/RP/2272/20. AMK has received this grant.

Conflicts of interest/Competing interests:

all authors declare no conflict of interest

Availability of data and material (data transparency):

data will be published in research gate

Code availability (software application or custom code):

Not applicable

Ethics approval (include appropriate approvals or waivers):

Ethical approval for the study was obtained from the Ethical Review Committee of Sri Lanka Medical Association ((Protocol No: ERC/21-001).

Consent to participate (include appropriate statements):

Not applicable in this retrospective study

Consent for publication (include appropriate statements):

NA

Author contribution

IK- Conceptualization, study design, data acquisition and management, analysis, interpretation, drafting and editing manuscript, approval of the final version

BAG - Conceptualization, data acquisition, critically analyzing manuscript, approval of the final version

AMK - Data acquisition, critically analyzing manuscript, approval of the final version

References

1. Parasher A. COVID-19: Current understanding of its pathophysiology, clinical presentation and treatment. *Postgrad Med J.* 2021;97:312–20.
2. Das S, Anu KR, Raosaheb S, Nitin A, Pandey A. Role of comorbidities like diabetes on severe acute respiratory syndrome coronavirus-2: A review. *S Life Sciences.* 2020;258:118202. <https://doi.org/10.1016/j.lfs.2020.118202>.
3. Fisman DN, Tuite AR. Evaluation of the relative virulence of novel SARS-CoV-2 variants: a retrospective cohort study in Ontario, Canada. *Can Med Assoc J.* 2021;193:E1619-25.
4. Ehtioui A, Zouch W, Ghorbel M. Detection Methods of COVID-19. *SLAS Technology* 2020;1 -7. <https://doi.org/10.1177/2472630320962002> 2020.
5. Wasilewski PG, Mruk B, Mazur S, Pótorak-Szymczak G, Sklinda K, Walecki J. COVID-19 severity scoring systems in radiological imaging - A review. *Polish J Radiol.* 2020;85:e361-8.
6. Garg PK, Khera PS, Saxena S, Sureka B, Garg MK, Nag VL, et al. Chest-x-ray-based scoring, total leukocyte count, and neutrophil-to-lymphocyte ratio for prediction of covid-19 in patients with severe acute respiratory illness. *Turkish Thorac J.* 2021;22:130–6.
7. Yasin R, Gouda W. Chest X-ray findings monitoring COVID-19 disease course and severity. *Egypt J Radiol Nucl Med.* 2020;51:193.
8. Jacobi A, Chung M, Bernheim A, Eber C. Portable chest X-ray in coronavirus disease-19 (COVID-19): A pictorial review. *Clin Imaging.* 2020;64:35–42. doi:10.1016/j.clinimag.2020.04.001.
9. Rousan LA, Elobeid E, Karrar M, Khader Y. Chest x-ray findings and temporal lung changes in patients with COVID-19 pneumonia. *BMC Pulm Med.* 2020;20:245. <https://doi.org/10.1186/s12890-020-01286-5>.
10. Borghesi A, Maroldi R. Short communication covid 19 outbreak in Italy?: experimental chest X ray scoring system for quantifying and monitoring disease progression. *La radiologia medica* 2020;509-13. <https://doi.org/10.1007/s11547-020-01200-3>.
11. Balbi M, Caroli A, Corsi A, Milanese G, Surace A, Di Marco F, et al. Chest X-ray for predicting mortality and the need for ventilatory support in COVID-19 patients presenting to the emergency department. *Eur Radiol.* 2021;31:1999–2012.

12. Yasin R, Gouda W. Chest X-ray findings monitoring COVID-19 disease course and severity. *Egypt J Radiol Nucl Med.* 2020;51:193. <https://doi.org/10.1186/s43055-020-00296-x>.
13. Ergönel Ö, et al., National case fatality rates of the COVID-19 pandemic, *Clinical Microbiology and Infection*, <https://doi.org/10.1016/j.cmi.2020.09.024>.
14. Tuddenham WJ. Glossary of terms for thoracic radiology: Recommendations of the nomenclature committee of the Fleischner society. *Am J Roentgenol.* 1984;143:509–17.
15. Kodikara I, Galabada BA, Hettiarachchi NS. The mortality predicting ability of customized chest X-ray severity scoring systems in Covid-19 pneumonia. Under review.
16. Pan F, Ye T, Sun P, Gui S, Liang B, Li L, et al. Time course of lung changes at chest CT during recovery from Coronavirus disease 2019 (COVID-19). *Radiology.* 2020;295:715–21.
17. Lu S, Xing Z, Zhao S, Meng X, Yang J, Ding W, et al. Different appearance of chest CT images of T2DM and NDM patients with COVID-19 pneumonia based on an artificial intelligent quantitative method. *Int J Endocrinol.* 2021;2021:6616069. <https://doi.org/10.1155/2021/6616069>.
18. Huang C, Wang Y, Li X, et al. "Clinical features of patients infected with 2019 novel coronavirus in Wuhan, China" *The Lancet.* 2020;395(10223):497–506.
19. McGroder CF, Zhang D, Choudhury MA. et al Pulmonary fibrosis 4 months after COVID-19 is associated with severity of illness and blood leucocyte telomere length. *Thorax.* 2021;76:1242–45.
20. Rai DK, Sharma P, Kumar R. Post Covid pulmonary fibrosis. Is it real threat? *Indian journal of tuberculosis.* 2021;68:330–1.
21. Lomoro P, Verde F, Zerboni F, et al. COVID-19 pneumonia manifestations at the admission on chest ultrasound, radiographs, and CT: single-center study and comprehensive radiologic literature review. *Eur J Radiol Open.* 2020;7:100231. <https://doi:10.1016/j.ejro.2020.100231>.
22. Chen N, Zhou M, Dong X, et al. Epidemiological and clinical characteristics of 99 cases of 2019 novel coronavirus pneumonia in Wuhan, China: a descriptive study. *Lancet.* 2020;395(10223):507–13. [https://doi:10.1016/S0140-6736\(20\)30211-7](https://doi:10.1016/S0140-6736(20)30211-7).
23. Yoon SH, Lee KH, Kim JY, et al. Chest radiographic and CT Findings of the 2019 novel Coronavirus disease (COVID-19): analysis of nine patients treated in Korea. *Korean J Radiol.* 2020;21:494–500.
24. Setiawati R, Widyaningroem A, Handarini T, Andriani J, Tanadi MR, Kamal IH. Modified chest x-ray scoring system in evaluating severity of COVID-19 patient in Dr. Soetomo General Hospital Surabaya, Indonesia. *Int J Gen Med* 2021;2407–12.
25. Li J, Yu X, Hu S, Lin Z, Xiong N, Gao Y. COVID-19 targets the right lung. *Critical care.* 2020;24:339. <https://doi.org/10.1186/s13054-020-03033-y>.

Figures

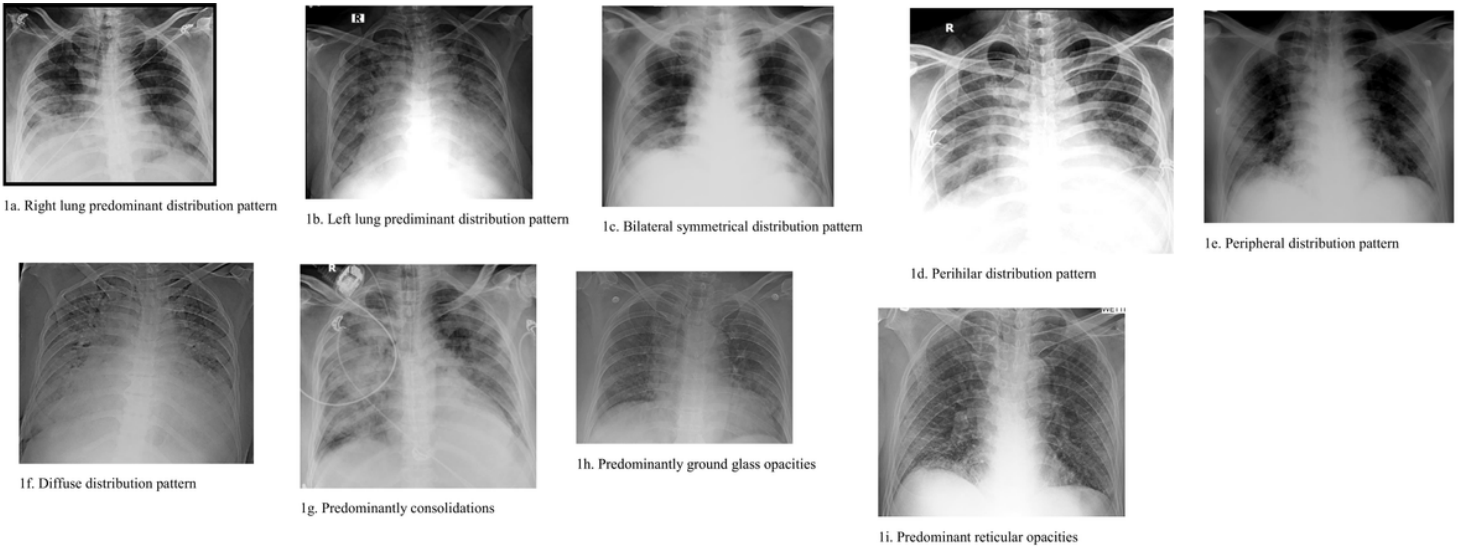


Figure 1

Please See image above for figure legend.

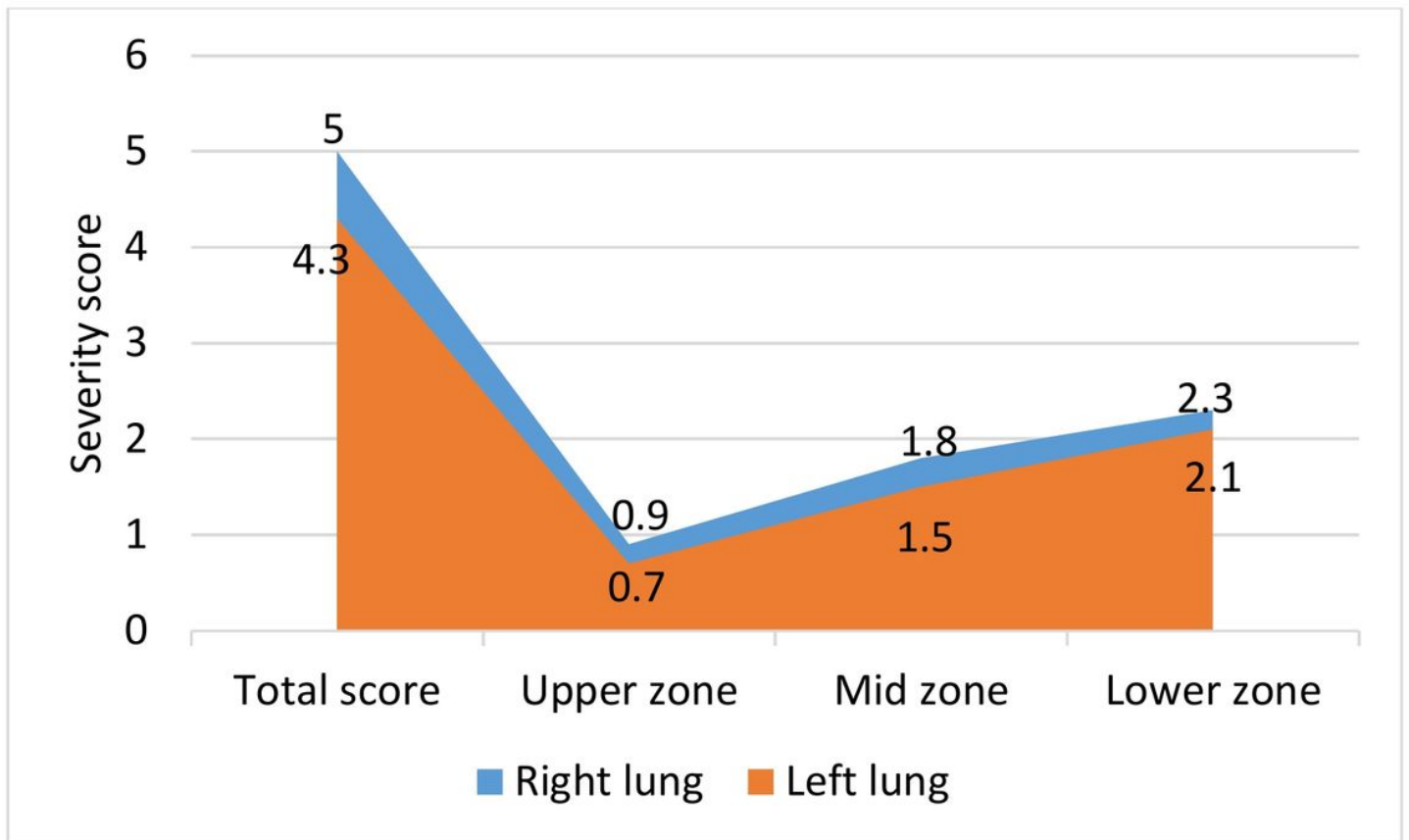
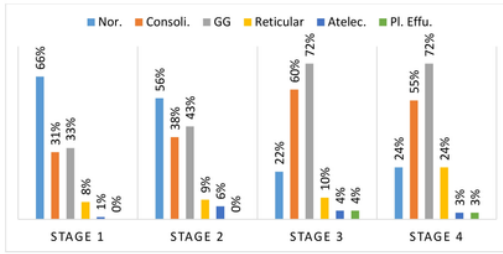


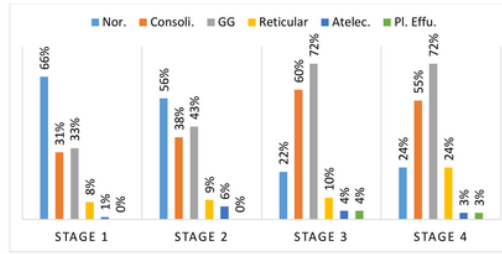
Figure 2: Severity of lung involvement in Covid-19 pneumonia

Figure 2

Please See image above for figure legend.



3a. Spatial distribution of opacities in the lungs



3a. Spatial distribution of opacities in the lungs

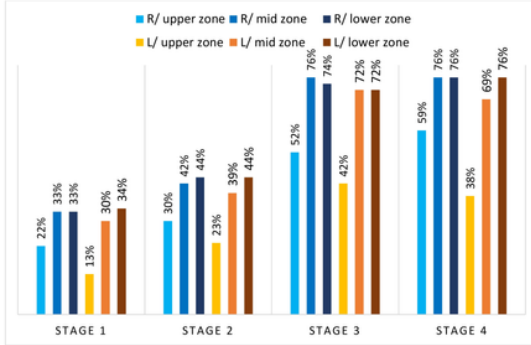


Figure 3c. Distribution of opacities in the lung zones

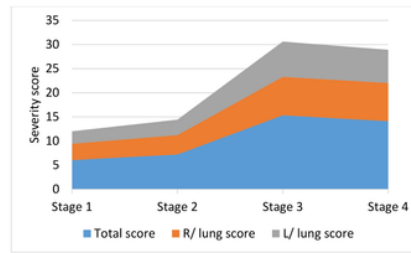


Figure 3d. Distribution of severity score in the lungs

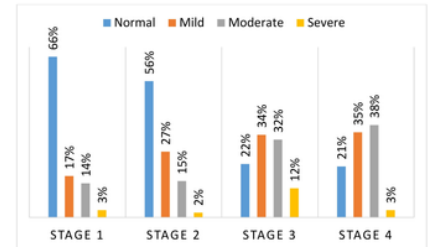


Figure 3e. Distribution of radiological severity according to the disease stage

Figure 3

Please See image above for figure legend.

Supplementary Files

This is a list of supplementary files associated with this preprint. Click to download.

- [STROBEchecklistv4combinedPlosMedicine.pdf](#)